The Homotropenylium Cation: A System with a Pinched π Ring Current †

Mark Lillington,[1] Remco W. A. Havenith,[2,3] Patrick W. Fowler,[1]* Jon Baker[4,‡] and Leonardus W. Jenneskens[5]*

[1]*Department of Chemistry, University of Sheffield, Sheffield S3 7HF, U.K*

[2]*Theoretical Chemistry, Zernike Institute for Advanced Materials, Rijksuniversiteit Groningen, Nijenborgh 4, 9747 AG Groningen, The Netherlands.*

[3]*Ghent Quantum Chemistry Group, Department of Inorganic and Physical Chemistry, Ghent University, Krijgslaan 281 – Building S3, B-9000 Gent, Belgium.*

[4]*Parallel Quantum Solutions, 2013 Green Acres Road, Suite A Fayetteville, Arkansas 72703, U.S.A.*

[5]*Organic Chemistry and Catalysis, Debye Institute for Nanomaterials Science, Utrecht University, Universiteitsweg 99, 3584 CG Utrecht, The Netherlands.*

Correspondence to: Patrick W. Fowler; e-mail P.W.Fowler@sheffield.ac.uk and Leonardus W. Jenneskens; email l.w.jenneskens@uu.nl

‡ Deceased 14 January 2014.

Acknowledgements

This paper is dedicated by his co-authors to the memory of Dr. Jon Baker, our colleague, collaborator and friend. Contract/grant sponsor: National Science Foundation; grant number CHE-0515922 (J. B.). R.W.A.H. acknowledges Prof. Dr. R. Broer (University of Groningen, The Netherlands) for fruitful discussions and the Zernike Institute for Advanced Materials of the University of Groningen for financial support (Dieptestrategie program). P.W.F. thanks the Royal Society/Leverhulme Trust for a Senior Research Fellowship during which this work was completed.

Graphical Abstract

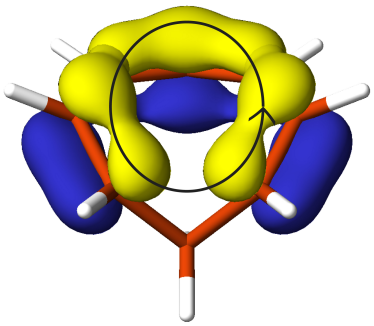

A diatropic ring current with a distinctive pinched topology: from classic p_π-p_π overlap (seven-carbon perimeter) to nearly pure p_σ-p_σ overlap in the gap.

Abstract

The homotropenylium cation (**1**, $C_8H_9^+$) is a key species in the discussion of homoaromaticity. Constrained optimizations around the minimum structure have been performed, varying the size of the gap spanned by the CH_2-bridge and optimising all other geometrical parameters. At each bridging distance, *ab initio* current-density maps have been calculated and plotted using the ipsocentric approach. Analysis of the maps, including decomposition into localized orbital contributions, gives a clear indication of a global diatropic ring current passing through the gap. The change in p_π-p_π interaction, from conventional π overlap around the conjugated seven-carbon perimeter to σ overlap (p_σ-p_σ) in the gap, results in a distinctive pinched topology, with two streams of current pinched down into one for part of the circuit. This ring current is diatropic and therefore the species **1** is aromatic on the magnetic criterion.

Introduction

In this paper we re-visit the homotropenylium cation (**1**, $C_8H_9^+$), a key structure in the long-standing discussion of homoaromaticity.[1,2] We will address its homoaromatic character from the point of view of the magnetic criterion of aromaticity,[3-6] namely the ability of a cyclic π-conjugated system to support a diatropic ring current induced by an external magnetic field. We apply the well documented ipsocentric approach for the *ab initio* computation and visualisation of currents induced by an external magnetic field.[7-11] It will be shown that, in spite of the interruption of π conjugation by the CH_2 bridge, the homotropenylium cation (**1**) sustains a six π-electron global diatropic ring current, albeit with a distinctive topology. As a consequence of the change in p_π-p_π interaction from conventional π (sideways-on) overlap within the conjugated C7 chain to σ (end-on) overlap in the gap, the ring current is pinched down from a pair of parallel circulations on both faces of the conjugated framework into a single stream crossing the gap. Despite this unusual feature, the species **1** meets the definition of π aromaticity on the magnetic criterion and so can be said to exhibit homoaroamaticity.

Computational details

Previous computational studies of **1** have shown strong dependence of the results on the level of theory. In particular, RHF calculations of the profile of total energy (E_{tot} in Hartree) versus the gap distance *R* (C1···C7 in Å) give double minima, which reduce to a single minimum at MP2 and higher levels.[12-13] Here we use optimization at the B3LYP/6-31G** level as a simple way of generating a profile with a single minimum.[14-15]

As we are interested in investigating the aromaticity of **1** and its dependence on the geometry of the CH_2-bridge, a sequence of C_s-symmetric structures with constrained *R* (C1···C7) distances (and all other parameters optimized) was also generated. The resulting energy profiles of total energy (E_{tot} in Hartree) *versus* the *R* (C1···C7) distance (in Å) are shown in the Electronic supplementary information (ESI: Fig. S1 and Table S1). As verified by Hessian calculations, this curve has a single minimum for a C_s-symmetric structure with *R* (C1···C7) = 2.127 Å. The overall flatness of the potential energy surface near the equilibrium *R* (C1···C7) distance is attested by MP2(full)/6-31G* calculations[13] where a shallow single-well potential energy curve with a minimum at *R* (C1···C7) = 2.03 Å and stretching constant *k*(C1···C7) of only 0.2 mdyn/Å was found.[16] At the present DFT B3LYP/6-31G** level of theory, the energy profile is also very shallow, and has a shift in the minimum of *ca.* 0.1 Å and somewhat greater curvature (*k*(C1···C7) = 0.3 mdyn/Å).

At selected points along the B3LYP/6-31G** energy profile, a calculation of induced current density was performed using GAMESS-UK[15] and SYSMO[18] using the *ipsocentric* DFT approach[17] at the CTOCD-*DZ*/B3LYP/6-31G**//B3LYP/6-31G** level of theory.

Results and discussion

(i) The homotropenylium cation 1, $C_8H_9^+$

A possible problem with description of non-planar molecules is that no formal separation of σ and π orbitals is available. However, analysis of the geometry of the minimum energy structure and nearby C_s-symmetric structures suggests that the separation remains approximately valid for **1**.[12, 13, 19] Bond lengths within the conjugated system C1-C2 …. C6-C7 are all close to typical 'aromatic' values and, significantly, sums of valence angles for these seven centres are all close to 360°, indicating formal sp^2 hybridization (Fig. 1), even if directed differently in space. Orthogonality defines a full set of local (though not necessarily parallel) p_π-orbitals from which π-like molecular orbitals can be constructed. This is the basis of our definition of π–like orbitals and currents (see below).

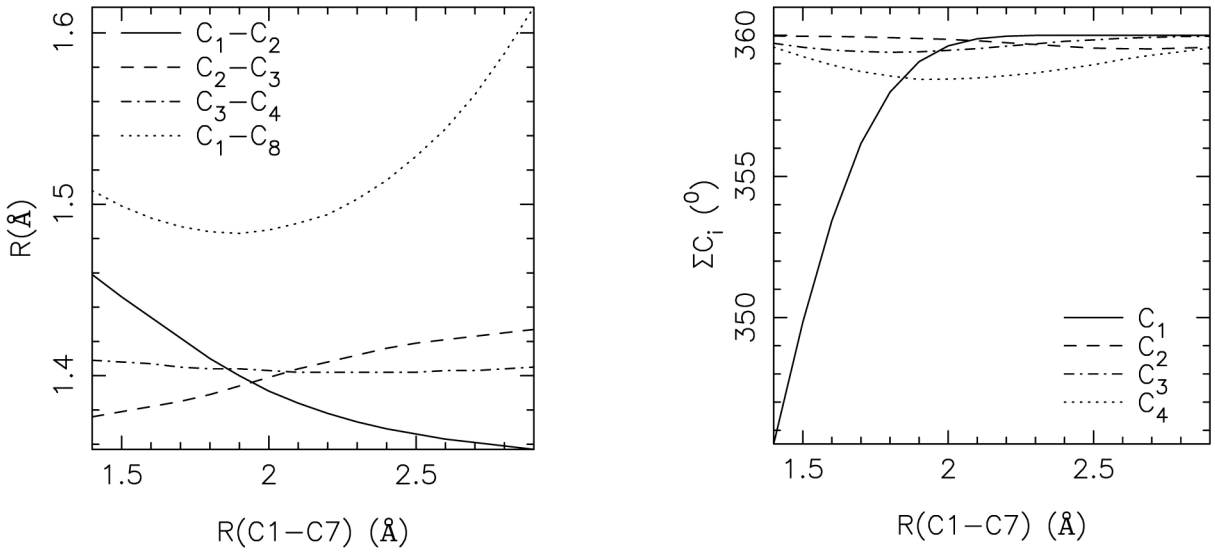

Fig. 1. Variation of bond lengths (left) and bond angle sums (right) in the homotropenylium cation (**1**, $C_8H_9^+$) as a function of the constrained distance *R* (C1···C7) at the B3LYP/6-31G** level of theory (See also Fig. 2**)**.

The data presented in Fig. 1 (See also ESI Table S1) show that only the C1-C8 and the C1-C2 bond distances change significantly upon changing the C1···C7 distance. For large distances *R* (C1···C7) ≥ 2.4 Å, the C1-C2 bond approaches the bond length of a typical double bond, while the C1-C8 bond distance lengthens. Furthermore, the change in the sum of the valence angles (∑(∠C1(C7))º) around C1(C7) reflects a change in hybridisation from 'sp^3-like' to 'sp^2-like' character at large C1···C7 distances. At the B3LYP/6-31G** optimised geometry, this sum of angles (∑(∠C1(C7))º) already closely approximates 360º, indicating that at this geometry C1 and C7 are already sp^2 hybridised.[12] The geometry is characteristically 'aromatic' in a range of ± 0.2 Å or around the minimum. The sums of the other angles are all close to 360º, indicating the near sp^2 hybridisation of the remaining carbon atoms.

A related problem affecting the treatment of magnetic response for non-planar molecules such as **1**, is that the direction of the applied magnetic field inducing the ring current is not uniquely defined. This hampers an unambiguous analysis of the current density in terms of selection rules for purely rotationally or translationally allowed excitations between occupied-to-unoccupied delocalised canonical molecular orbitals (CMOs).[9,10] Here we choose a reference plane based on the near co-planarity of the main conjugated system[12,19,20] and take the common plane of centres C1, C3, C5 and C7 (See Fig. 2), the normal to which implies a direction of the magnetic field for any choice of the distance *R* (C1···C7). Plotting current density maps parallel and perpendicular to this plane

will then have the advantage of providing unobstructed views of current in the C1 to C7 gap.

Characterisation of orbital contributions to the maps can be obtained, by using a localised description.[21] The π-like orbitals of **1** can be identified via the Pipek-Mezey procedure,[22, 23] where we look for those localised molecular orbitals (LMO) that have a nodal surface matching the local sp^2 geometry implied by the bond angles at the carbon centres; contributions to the induced current density can then be calculated for each π-like LMO and summed to produce the total π-current. A significant feature of this approach is that it gives an internal magnetic criterion of localizability, based on economy of description. Intrinsically delocalised electrons yield localised orbitals that display disjoint *open* flow lines, and their currents are better described with canonical molecular orbitals, whereas localisable electrons yield *closed-loop* patterns directly on orbital localisation.

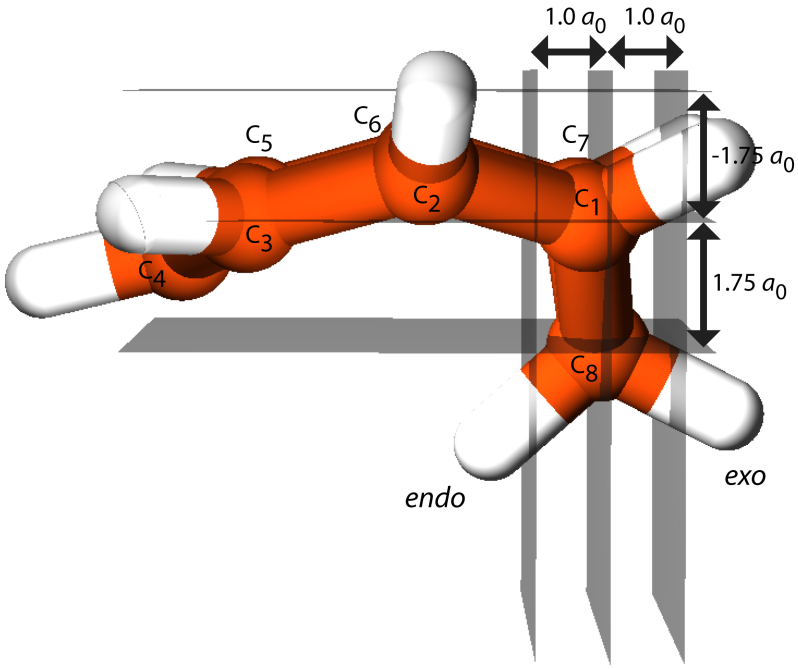

Fig. 2. Planes used for the plotting of the current density maps of (C_s-constrained) homotropenylium cation (**1**, $C_8H_9^+$). The plane (C1, C3, C5, C7) is used as a reference 'σ-plane' for maps of the conventional π current in planes above and below, and the plane (C1, C8, C7) is a reference for investigating the π-like current across the C1···C7 gap, *inside* ('*endo*') and *outside* ('*exo*') the molecular framework.

(ii) Current-density maps for the homotropenylium cation (1, $C_8H_9^+$)

To establish whether the homotropenylium cation (**1**) in its B3LYP/6-31G** global minimum (C_s-symmetric, with *R* (C1···C7) = 2.127 Å) sustains an induced diatropic ring current in an external magnetic field, DFT current-density maps[17] were calculated using GAMESS-UK[15] and SYSMO.[18] Maps are plotted at positive (towards the CH_2 unit on position C8) and negative (away from the CH_2 unit on position C8) heights (in bohr, a_0) from the reference plane (Fig. 2). Maps for negative height are expected to be 'cleaner' in that they will not intersect CH_2 bonds and should exhibit both π-type currents and the current, if any, present in the CH_2-bridged gap.

An initial plot of the map of total (all-orbital, 'σ+π') induced current density at a plotting distance of -1.75 a_0 below the reference plane shows evidence of a continuous global current in the diatropic sense (Fig. 3(a)), but this is partially obscured by other local features. Pipek-Mezey localisation[22] followed by inspection of nodal characteristics enables the assignment of eight C 1s cores, eight local σ-type C-C bonds, nine local σ-type C-H bonds and three orbitals of π-like character (Fig. 4). Decomposition of the total current density (Fig. 3(a)) into contributions from σ-type and π-type localised orbitals then shows that the global circulation comes from contributions of the set of three π-like orbitals, including one tha t (Fig. 3(b)). Comparison of the two plots leads to the conclusion that the bulges seen at the C2 and C6 positions in the total current density plot (See Fig. 3a) arise from the two C-H bonds that pass close to the plotting plane. The remaining 25 orbitals do not contribute to the global current (Fig. 3c).

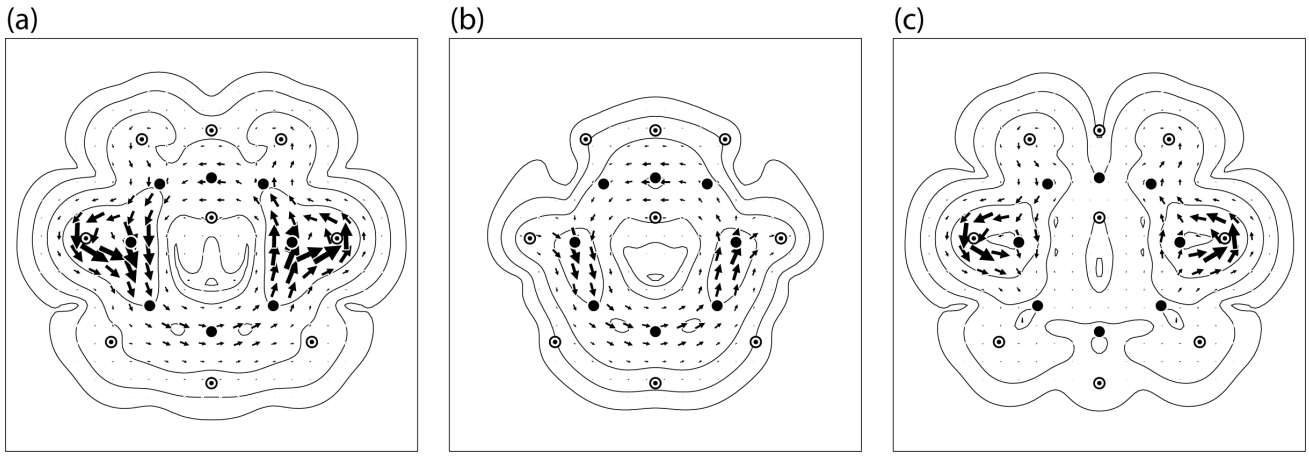

Fig. 3. Current-density maps for the B3LYP/6-31G** optimised homotropenylium cation (**1**, $C_8H_9^+$ with *R* (C1···C7) 2.127 Å). Contributions from (a) all orbitals ('σ+ π'); (b) localised 'π-like'

orbitals; (c) all orbitals except the three localised 'π-like' orbitals; All plots are at a height of -1.75 a_0, *e.g.* below the reference plane C1, C3, C5, C7 (See Fig. 2).

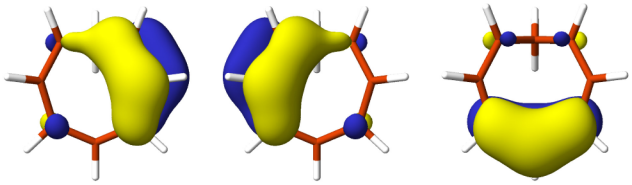

Fig. 4. Plots of the localised 'π-like' orbitals that contribute to the 'π-like' current of Fig. 3b. The molecular framework is viewed from underneath.

The π current-density map obtained in this way shows a patchy global circulation with holes in the C1-C2 and C6-C7 regions (Fig. 3(b)). However, it should be remembered that the arrows in the map represent the component of current density resolved into the plotting plane. Current can dip in and out of the plotting plane.[24] That the holes in the maps are caused by such changes in current direction becomes clear when the same decomposition is applied at different plotting heights: the pattern of global diatropic circulation shows a tendency to fill in as the plotting plane is made to approach and then pass through the reference plane C1, C3, C5, C7 (Fig. 5).

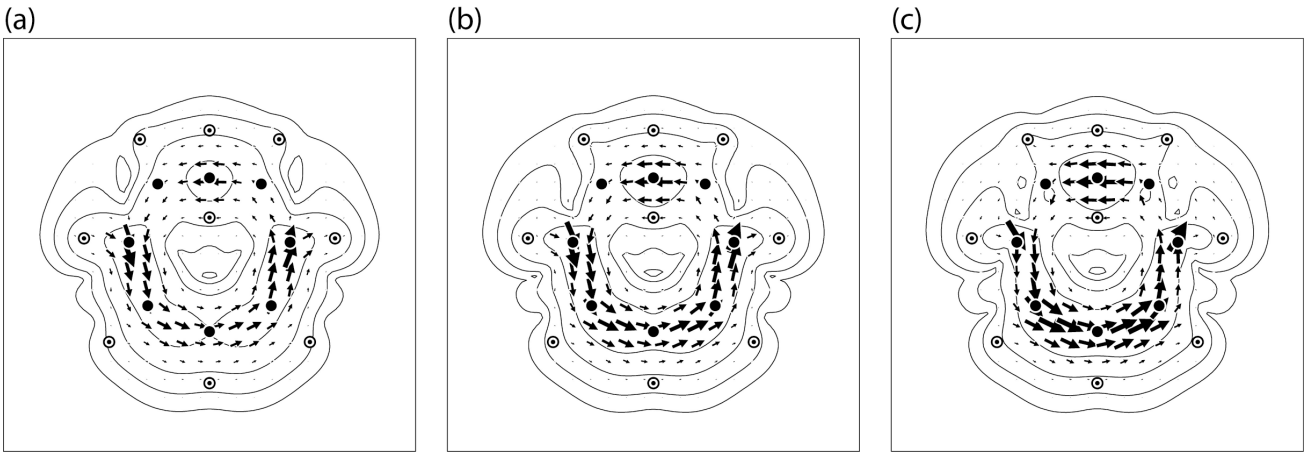

Fig. 5. Current-density maps for the B3LYP/6-31G** optimised homotropenylium cation (**1**, $C_8H_9^+$ with *R* (C1···C7) 2.127 Å), showing the continuity of the global diatropic π-circulation. The orbital decomposition is equivalent to that used in Fig. 3(b), but with plotting heights of (a) -1.5 a_0 (j_{max} = 0.049 a.u.), (b) -1.25 a_0 (j_{max} = 0.067 a.u.), and (c) -1 a_0 (j_{max} = 0.088 a.u.) below the reference plane C1, C3, C5, C7 (See Fig. 2). All other plotting conventions remain the same; note that for B3LYP/6-31G** benzene at 1 a_0 j_{max} = 0.079 a.u..[17]

We now focus on the character of the induced current contributions across the CH_2-bridged gap *R* (C1···C7). The contribution from the three localised π-like orbitals is shown in Fig. 6, in which the current is mapped in a plane 1 a_0 from C8 *inside* (‘*endo’*) the ring. What is clear from the plot is that this contribution crosses a region of space where there is no formal bond. This π-like current across the CH_2 gap is interpreted as arising from the ‘end-on’ overlap of p_π-orbitals on C1 and C7, with this overlap leading to a single maximum in current density below the molecular reference plane C1, C3, C5, C7 (See Fig. 2). Comparison of ‘*endo’* and ‘*exo’* plots (Fig. 6 and ESI Fig. S2, respectively) shows that this overlap contribution under the CH_2 bridge is more intense towards the inside of the ring, as is expected from the directions of the overlapping pair of p_π-orbitals.

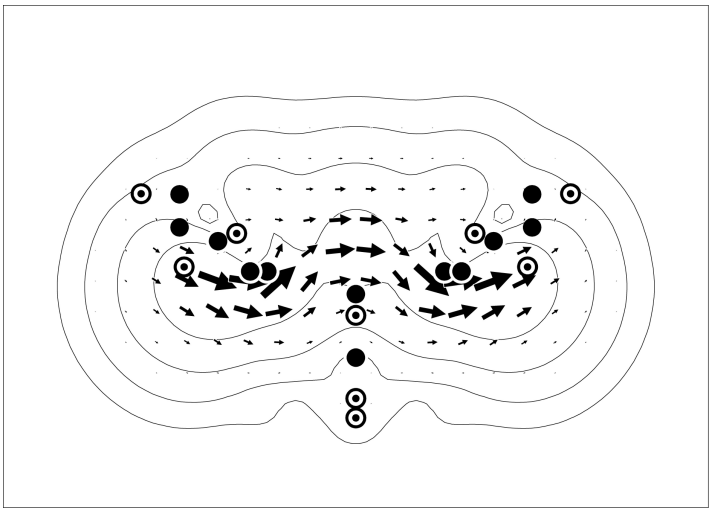

Fig. 6. A current-density map showing the current in the region of the CH_2-bridged gap between C1 and C7 in the B3LYP/6-31G** optimised homotropenylium cation (**1**, $C_8H_9^+$ with *R* (C1···C7) 2.127 Å). The total contributions from the three π-like localised occupied orbitals is shown. The current is mapped in a plane 1 a_0 from C8 *inside* (‘*endo’*) the ring, perpendicular to both the reference plane C1, C3, C5, C7 (See Fig. 2) and the C_s symmetry plane. The external magnetic field is parallel to the plotting plane.

The partial snapshots of the current distribution (Fig. 7) are integrated into a single global description in the sequence shown in Fig. 8**,** where the π contribution to current density and corresponding slices through the π charge density are plotted in vertical planes that constitute a kind

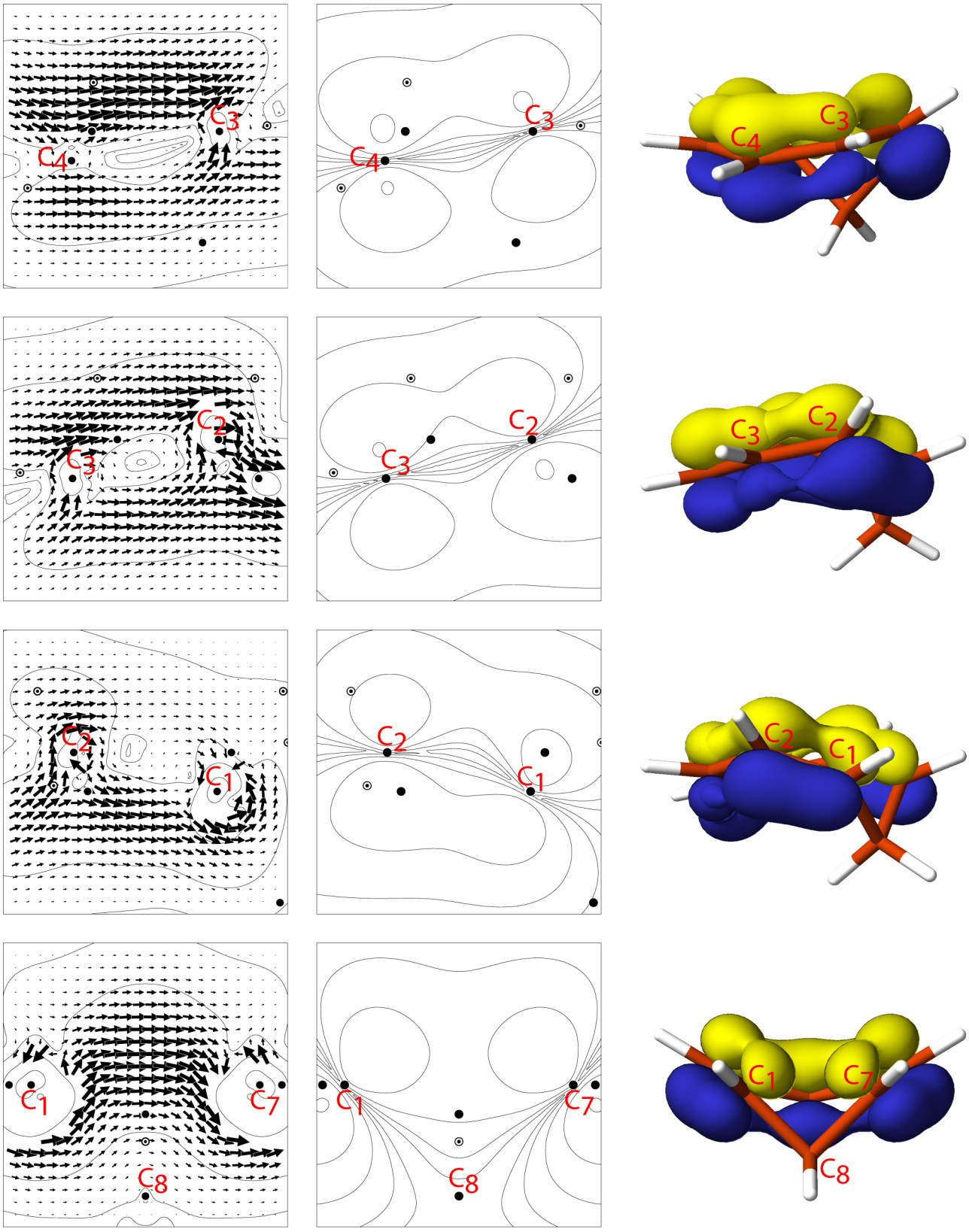

Fig. 7. Sideview of the 'π-like' current (left) plotted in a plane perpendicular to the reference plane C1, C3, C5, C7 (See Fig. 2) and containing the two carbon atoms of interest. The electron density of the contributing molecular orbitals is plotted in the same plane on the right.

of 'boundary fence' around the molecule containing the C4-C3, C3-C2, C2-C1 and *R* (C1···C7) bonds on successive panels of the fence. As we travel around the ring and approach the CH_2 bridge, the two lobes of π ring current approach more closely, tilt, and finally become pinched into one at C2 and pass under the reference plane and into the C1···C7 gap as a single stream of current. The close correspondence between the contours of current density and those of the density of the π orbitals formed by overlap of local p_π functions is clear (Fig. 8). The main conclusion is that there is a 'genuine' diatropic homoaromatic ring current flowing across the CH_2-bridged gap,[25] which has a distinctive pinched topology as dictated by orbital overlap, and as Fig. 9 shows, the pinched ring current is robust against changes of the geometry within the vicinity of the minimum.[12,13]

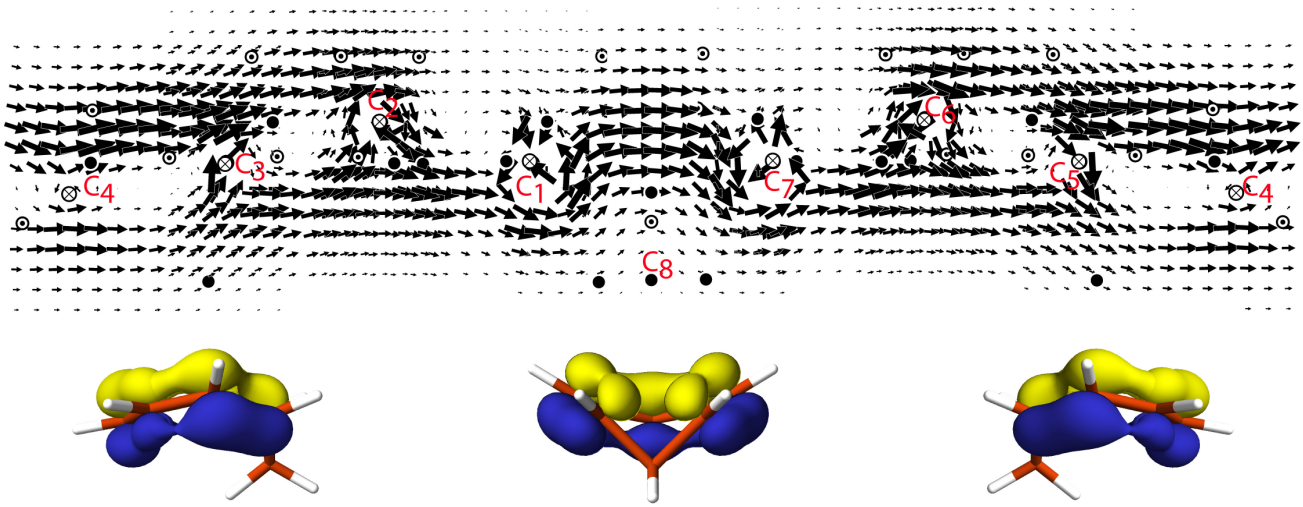

Fig. 8. Combination of side view plots of the 'π-like' currents (Fig. 7) to show a panorama of the flow of current all the way around the ring in **1**. The 'π-like' orbitals combined are shown to show the orientation of the molecule.

It is noteworthy that the panorama of the flow of current shown in Fig. 8 is fully in line with the results of a POAV2/3D-HMO[25] analysis on the B3LYP/6-31G** optimised structure of the homotropenylium cation (**1**, $C_8H_9^+$, C_s-symmetric with *R* (C1···C7) = 2.127 Å). Whereas two-center POAV2/3D-HMO analysis of the homoaromatic bond C1···C7 reveals a contribution of predominantly pure p_σ-p_σ overlap (0.098 with a reduced resonance integral $\rho_{1,7}^B = 0.558$ (scaled by the nearest-neighbour p_π-p_π overlap integral in benzene[12,19,25])), nearly pure p_π-p_π overlap is found for the conjugated bonds (C1-C2/C7-C6 p_π-p_π overlap 0.2467 with the reduced resonance integral $\rho_{1,2/7,6}^B = 1.004$, C2-C3/C6-C5 p_π-p_π overlap 0.2225 with the reduced resonance integral $\rho_{2,3/6,5}^B = 0.906$, and C3-C4/C5-C4 p_π-p_π overlap 0.2368 with the reduced resonance integral $\rho_{3,4/5,4}^B = 0.963$

(See also Fig. 2). Similar results were obtained by Haddon, albeit using a less reliable RHF optimised global minimum of the homotropenylium cation (**1**).[12,19]

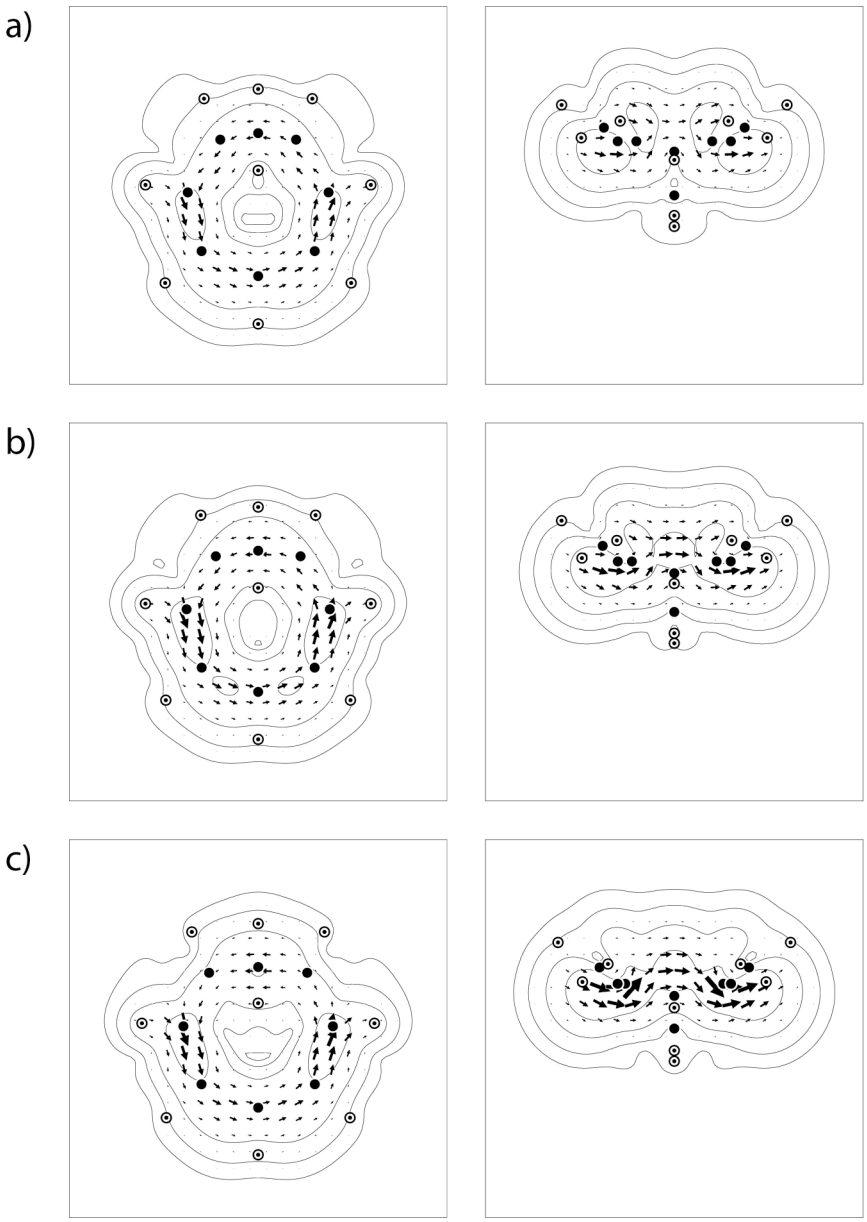

Fig. 9. Current-density maps for the homotropenylium cation (**1**, $C_8H_9^+$) as a function of the bridged distance *R* (C1···C7); a) *R* (C1···C7) = 1.7 Å, b) *R* (C1···C7) = 1.9 Å and c) *R* (C1···C7) = 2.2 Å.

Our claim for homoaromaticity of homotropenylium cation (**1**, $C_8H_9^+$) rests on the calculation of a ring current attributable to the p_π subsystem of the molecule. Whilst compelling in itself, this claim should also be compatible with evidence from approaches that eschew the use of orbitals. One such approach is topological analysis of the electron localisation function (ELF),[26] which partitions molecular space into 'basins', and identifies electron delocalisation with variance in basin

populations. As electron delocalisation is a necessary condition for existence of ring current in the ipsocentric picture, it is gratifying to note that ELF analysis for **1**[27] is reported to find 'complete cyclic electron delocalisation', supporting an attribution of no-bond homoaromaticity to this system.

In the ipsocentric picture, delocalisation of itself is not sufficient to guarantee a current. Calculation of *total* induced current in homotropenylium cation has also been reported.[28] The calculation uses the GIMIC method,[30] where regions of net diatropic and paratropic flow are identified by integration over user-defined spatial domains. Typically, diatropic flow is found on the outside of a molecular ring (whether saturated or unsaturated) and paratropic flow in its interior.[28] When the interpretation that orbital analysis provides is set aside, as in the GIMIC approach, then aromaticity, non-aromaticity and anti-aromaticity emerge somewhat mysteriously from the integration procedure as particular patterns of partial cancellation of internal and external currents.[28] The GIMIC calculations show **1** as supporting an internal paratropic circulation skirting the CH_2 bridge region, and an external diatropic current that flows under and outside the bridge. The same spatial pattern of total current is given a transparent and transferable interpretation in our ipsocentric orbital model. Much of the cancellation in total current is seen to arise simply from single-bond circulations within the localised CC/CH σ system: paratropic on the inside, diatropic on the outside.[30] The π system is left, delivering the net diatropic ring current of the conventional aromatic, the paratropic ring current of the conventional anti-aromatic, and the localised lone-pair currents of non-aromatic systems such as borazine.[31] In the case of **1**, this π current survives in modified form, with an unusual spatial distribution, but still with a clearly defined origin within the electronic structure according to our approach.

Conclusion

It has been shown by direct computation and mapping of the induced current density that the homotropenylium cation (**1**, $C_8H_9^+$) supports a diatropic ring current, and should therefore be considered as (homo)aromatic on the magnetic criterion. A π-like ring current is identified within the full current density by appropriate use of localised molecular orbitals. It jumps the gap spanned by the CH_2 bridge, is robust against widening of the gap, and has a distinctive pinched topology, where the two streams of a conventional π ring current in the conjugated part of the molecular circuit squeeze down into one as the current dips into the gap spanned by the CH_2-bridge. The calculations support the empirical POAV2/3D-HMO[25] analysis made many years ago by Haddon:[12,19] the overlap that supports the current changes is based on a chain of local p orbitals, from classic p_π-p_π interaction in the bonds remote from the bridge to an approach to pure p_σ-p_σ interaction in the gap.

Notes and References

† Electronic supplementary information (ESI) available: Fig. S1; RHF/6-31G** and B3LYP/6-31G** energy profiles of **1**, $C_8H_9^+$ (E_{rel} (in kcal/mol) *versus* the *R* (C1···C7) distance (in Å, Fig. S1). Fig. S2; a current-density map showing the current in the region of the CH_2-bridged gap between C1 and C7 in the B3LYP/6-31G** optimised homotropenylium cation (**1**, $C_8H_9^+$ with *R* (C1···C7) 2.127 Å) in a plane 1 a_0 from C8 *outside* (‘*exo’*) the ring, perpendicular to both the reference plane (C1, C3, C5, C7) and the C_s symmetry plane. B3LYP/6-31G** salient structural data of (constrained) optimised geometries of **1**, $C_8H_9^+$ (Table S1), B3LYP/6-31G** cartesian coordinates (in a_0) and E_{tot} (in Hartree) of fully optimised **1**, $C_8H_9^+$ (Table S2) and RHF/6-31G** cartesian coordinates (in a_0) and E_{tot} (in Hartree) of the global (Table S3) and local (Table S4) minima of **1**, $C_8H_9^+$.

‡ Deceased 14 January 2014.

1. V. I. Minkin, M. N. Glukhovstev, Ya. B. Simkin, Aromaticity and Antiaromaticity. Electronic and Structural Aspects, Wiley: New York 1994.
2. R. V. Williams, *Chem. Rev.* 2001, **101**, 1185-1204 and references cited.
3. L. Pauling, *J. Chem. Phys.*, 1936, **8**, 673-677.
4. F. London, *J. Phys. Radium*, 1937, **8**, 397-404.
5. J. A. Pople, *J. Chem. Phys.*, 1956, **24**, 1111.
6. P. v. R. Schleyer, C. Maerker, A. Dransfeld, H. Jiao and N. J. R. Eikema Hommes, *J. Am. Chem. Soc.*, 1996, **118**, 6317-6318.
7. T. A. Keith and R. F. W. Bader, *Chem. Phys Lett.* 1993, **210**, 223-231.
8. S. Coriani, P. Lazzeretti, M. Malagoli and R. Zanasi, *Theor. Chim. Acta*, 1994, **89**, 181-189.
9. E. Steiner and P. W. Fowler, *J. Phys. Chem. A*, 2001, **105**, 9553-9562.
10. E. Steiner and P. W. Fowler, *Chem. Commun.*, 2001, 2220-2221.
11. P. W. Fowler, E. Steiner, R. W. A. Havenith and L. W. Jenneskens, *Magn. Res. Chem.*, 2004, **42**, S68-S78.
12. R. C. Haddon, *J. Am. Chem. Soc.*, 1988, **110**, 1108-1112.
13. D. Cremer, F. Reichel and E. Kraka *J. Am. Chem. Soc.* 1991, **113**, 9459-9466.
14. PQS version 3.3, Parallel Quantum Solutions, 2013 Green Acres Road, Suite A, Fayetteville, AR 72703. Email: sales@pqs-chem.com; URL: http://www.pqs-chem.com.
15. GAMESS-UK: M. F. Guest, I. J. Bush, H. J. J. van Dam, P. Sherwood, J. M. H. Thomas, J. H. van Lenthe, R. W. A. Havenith and J. Kendrick, *Mol. Phys.*, 2005, **103**, 719-747.

16. See also: B. Reindl, T. Clark and P. v. R. Schleyer, *J. Phys. Chem. A*, 1998, **102** 8953-8963.
17. R. W. A. Havenith and P. W. Fowler, *Chem. Phys. Lett.*, 2007, **449** 347-353.
18. SYSMO Package: P. Lazzeretti and R. Zanasi (University of Modena, 1980) with additional routines for evaluation and plotting of current density by E. Steiner and P. W. Fowler, R. W. A. Havenith and A. Soncini.
19. See also: R. C. Haddon, *Acc. Chem. Res.*, 1988, **21** 243-249 and references cited.
20. R. W. A. Havenith, P. W. Fowler and L. W. Jenneskens, *Org. Lett.*, 2006, **8** 1255-1258.
21. E. Steiner, P.W. Fowler and R.W.A. Havenith, *J. Phys. Chem. A*, 2002, **106**, 7048-7056.
22. J. Pipek and P. G. Mezey, *J. Chem. Phys.*, 1989, **90**, 4916-4926.
23. See also: R. W. A. Havenith, L. W. Jenneskens, P. W. Fowler and E. Steiner, *Phys. Chem. Chem. Phys.*, 2004, **6**, 2033-2039.
24. A. Ligabue, A. Soncini and P. Lazzeretti, *J. Am. Chem. Soc.*, 2002, **124**, 2008-2014.
25. POAV/3D-HMO: R. C. Haddon, *J. Am. Chem. Soc.*, 1987, **109**, 1676-1685.
26. B. Silvi and A Savin, *Nature*, 1994, **371**, 683-686.
27. C. Lepetit, B. Silvi and R. Chauvin, *J. Phys. Chem. A*, 2003, **107**, 464-473.
28. H. Fliegl, D. Sundholm, S. Taubert, J. Jusélius and W. Klopper, *J. Phys. Chem. A*, 2009, **113**, 8668-8676.
29. J. Jusélius, D. Sundholm and J. Gauss, *J. Chem. Phys.*, 2004, **121**, 3952-3963.
30. E. Steiner and P.W. Fowler, *Phys. Chem. Chem. Phys.*, 2004, **6**, 261-272.
31. For example: A. Soncini, C. Domene, J. J. Engelberts, P. W. Fowler, A. Rassat, J. H. van Lenthe, R. W. A. Havenith and L. W. Jenneskens, *Chem. Eur. J.*, 2005, **11**, 1257-1266. J. J. Engelberts, R. W. A. Havenith, J. H. van Lenthe, L. W. Jenneskens and P. W. Fowler, *Inorg. Chem.*, 2005, **44**, 5266-5272.